



Data Article

A high-resolution multi-shell 3T diffusion magnetic resonance imaging dataset as part of the Amsterdam Ultra-high field adult lifespan database (AHEAD)



Max C. Keuken^{a,**}, Luka C. Liebrand^b, Pierre-Louis Bazin^{a,c}, Anneke Alkemade^a, Nikita van Berendonk^a, Josephine M. Groot^{a,d}, Scott J.S. Isherwood^a, Sarah Kemp^{a,e}, Nicky Lute^a, Martijn J. Mulder^f, Anne C. Trutti^{a,g}, Matthan W.A. Caan^{b,*}, Birte U. Forstmann^{a,*}

^a Integrative Model-based Cognitive Neuroscience Research Unit, University of Amsterdam, The Netherlands

^b Department of Biomedical Engineering and Physics, Amsterdam University Medical Centers, University of Amsterdam, Amsterdam, The Netherlands

^c Departments of Neurophysics and Neurology, Max Planck Institute for Human, Cognitive and Brain Sciences, Leipzig, Germany

^d Department of Psychology, UiT–The Arctic University of Norway, Tromsø, Norway

^e Sensorimotor Neuroscience and Ageing Research Lab, School of Psychological Sciences, College of Health and Medicine, University of Tasmania, Hobart, Australia

^f Experimental Psychology, Helmholtz Institute, Utrecht University, Utrecht, The Netherlands

^g Cognitive Psychology Unit and Leiden Institute for Brain and Cognition, Leiden University, Leiden, The Netherlands

** Corresponding author at: Integrative Model-based Cognitive Neuroscience Research Unit, University of Amsterdam, Nieuwe Achtergracht 129B, Postbus 15926, 1001 NK Amsterdam, the Netherlands

E-mail address: m.c.keuken@uva.nl (M.C. Keuken).

* Contributed equally

ARTICLE INFO

Article history:

Received 28 October 2021

Revised 7 March 2022

Accepted 16 March 2022

Available online 23 March 2022

Dataset link: [A high-resolution multi-shell 3T diffusion magnetic resonance imaging dataset as part of the Amsterdam Ultra-high field adult lifespan database \(AHEAD\) \(Original data\)](#)

Keywords:

DWI

MRI

Lifespan

Diffusion

3T

Multi-shell

ABSTRACT

In order to further our understanding of brain function and the underlying networks, more advanced diffusion weighted magnetic resonance imaging (DWI MRI) data are essential. Here we present freely available high-resolution multi-shell multi-directional 3 Tesla (T) DWI MRI data as part of the 'Amsterdam Ultra-high field adult lifespan database' (AHEAD). The 3T DWI AHEAD dataset include 1.28mm isotropic whole brain DWI data of 49 healthy adult participants between 18 and 90 years old. The acquired data include DWIs at three non-zero b-values (48 directions, b-value 700 s/mm²; 56 directions, b-value 1000 s/mm²; 64 directions, b-value 1600 s/mm²) including a total of twelve volumes with a b-value of 0 s/mm² (b0 volumes). In addition, eight b0 volumes with a reversed phase encoding direction were acquired to correct for distortions. To facilitate future use, the DWI data have been denoised, corrected for eddy currents, susceptibility-induced off-resonance field distortions, bias fields, and are skull stripped.

© 2022 The Author(s). Published by Elsevier Inc.

This is an open access article under the CC BY-NC-ND license (<http://creativecommons.org/licenses/by-nc-nd/4.0/>)

Specifications Table

Subject	Psychology
Specific subject area	Neuroscience: Cognitive
Type of data	Table MRI DWI data
How data were acquired	Philips 3T Ingenia CX MRI scanner using a dStream 32 channel receiver head coil.
Data format	Preprocessed
Parameters for data collection	Multi-shell (b700, b1000, b1600) multi-directional (resp. 48, 56 and 64 directions) with twelve b0 volumes, 1.28 mm isotropic resolution 3T diffusion MRI data. To correct for susceptibility-induced off-resonance field distortions eight b0 volumes with reversed phase encoding were acquired.
Description of data collection	As part of a larger data-collection effort, 54 healthy participants between the age of 18 and 90 were scanned on a 3T MRI scanner in the period of April 2019 and August 2020. The data acquisition took approximately an hour and included three diffusion weighted sequences: (1) 48 directions with a b-value of 700, (2) 56 directions with a b-value of 1000, and (3) the 64 directions with a b-value of 1600. To bypass memory limitations, the third sequence was split into two different volumes, each with 32 directions. The diffusion weighted sequences included twelve volumes with a b-value of 0. To enable the correction of susceptibility-induced off-resonance field distortions, eight additional volumes with a b-value of 0 were acquired with a reversed phase-encode direction. Due to technical issues, data of five participants were corrupted or incomplete. The final 3T DWI dataset contains data 49 participants and can be combined with previously published high-resolution multi-parameter 7T structural MRI data [1].
Data source location	Institution: Spinoza Center for Neuroimaging (https://www.spinozacentre.nl) City: Amsterdam Country: The Netherlands Latitude and longitude for collected data: 52°17'31.8"N 4°57'26.3"E

(continued on next page)

Data accessibility	Repository name: figshare.com Data identification number: N.a. Direct URL to data: https://uvaaus.figshare.com/projects/A_high-resolution_multi-shell_3T_diffusion_magnetic_resonance_imaging_dataset_as_part_of_the_Amsterdam_Ultra-high_field_adult_lifespan_database_AHEAD_/125377 Direct URL to the MRI exam card parameters used to acquire the data: DOI 10.17605/OSF.IO/ZVXHW Direct URL to the code used to process the data: DOI 10.17605/OSF.IO/ZVXHW
Related research article	Alkemade, A., Mulder, M., Groot, J., Isaacs, B., van Berendonk, N., Lute, N., Isherwood, S., Bazin, P.-L., & Forstmann, B. U. (2020). The Amsterdam Ultra-high field adult lifespan database (AHEAD): A freely available multimodal 7 Tesla submillimeter magnetic resonance imaging database. <i>NeuroImage</i> , 221, 117200.

Value of the Data

- The dataset entails a high-resolution multi-shell multi-directional 3T DWI acquisition that can be combined with multi-contrast 7T ultra-high field (UHF) structural MRI scans of the same participants that have already been made freely available.
- The dataset is relevant and freely available for researchers interested in structural networks in the healthy brain across the adult lifespan, as well as researchers interested in normative control groups for clinical cohorts.
- The DWI have been pre-processed with the following steps: denoising, eddy current correction, topup correction, N4 bias field correction, and skull stripping.
- The freely available dataset follows the Brain Imaging Data Structure (BIDS) specification and therefore supports the ease of future use.

1. Data Description

As part of a larger data-collection effort, 54 healthy participants between the age of 18 and 90 were scanned on a 3T MRI scanner in the period of April 2019 and August 2020. The DWI data included three diffusion weighted sequences: (1) 48 directions with a b-value of 700, (2) 56 directions with a b-value of 1000, and (3) the 64 directions with a b-value of 1600. The directional resolutions are provided in the *bvec* files per sequence and are further explained in [Table 2](#). Each diffusion-weighted scan was preceded by two *b0* scans that were later used with topup to correct for susceptibility-induced off-resonance field distortions. The *b700*, *b1000*, and *b1600* scans have identical acquisition parameters to the separate *b0* scans except an inverted

Table 1

Demographic information including the number of female and male participants per age group for whom diffusion-weighted data was acquired. All participants underwent a previous 7T structural MRI session which is described in [\[1\]](#). The average interval between the 7T structural MRI session and the 3T DWI session was 2.35 years (std. 0.23). The age group membership is based on the age at diffusion-weighted data acquisition and could therefore differ from the age group in the initial 7 Tesla structural data release.

Age Group (years)	Female	Male	Total
18-30	6	6	12
31-40	3	4	7
41-50	3	2	5
51-60	6	4	10
61-70	6	3	9
71-80	3	2	5
81-90	0	1	1
Total	27	22	49

Table 2

A short description of the shared files. Each of the 49 participants has a single folder which contains five different files: a binary brain mask, the processed DWI data in Nifti format with the corresponding bvals and bvecs files, and a text file containing the demographic information.

Participant ID	Data Type	Filename	Description
sub-{id number}	dwi	sub-{id number}_ses-03_ dwi_desc-Brain_mask.nii.gz	The binary mask of the brain estimated by <i>dwi2mask</i> and used to remove all facial features from the DWI data.
		sub-{id number}_ses-03_ dwi_desc-preproc_dwi.nii.gz	The concatenated DWI file of a single participant. Each concatenated DWI file consists of 180 volumes.
		sub-{id number}_ses-03_ dwi_desc-preproc_dwi.bvals	The corresponding b-values in s/mm^2 per DWI volume (12×0 , 48×700 , 56×1000 , 64×1600).
		sub-{id number}_ses-03_ dwi_desc-preproc_dwi.bvecs	The corresponding gradient table, stored in a bvecs format, per DWI volume. The file consists of 3 rows, corresponding to the x, y, and z component of the diffusion weighted gradient vector.
		sub-{id number}_ses-03_ demographics.txt	A text file that contains the participant id number, gender, and age group information.

fat shift direction (resp. anterior versus posterior), the number of directions and the b-value used. To further increase the number of b0 scans that could be used for topup, the b700 scan started and ended with a b0 volume. The b1000 scan started with a single and ended with 5 additional b0 volumes. The first half of the b1600 scan started and ended with a single b0 volume whereas the second half of the b1600 scan started with a single and ended with two b0 volumes. In total 8 b0 scans with an anterior shift direction and 12 b0 scans with a posterior shift were acquired. Due to technical issues, data of five participants were corrupted or incomplete. The freely available DWI data set has been pre-processed with the following steps: denoising, eddy current correction, topup correction, N4 bias field correction, and skull stripping. The final 3T DWI dataset contains 49 participants and can be combined with previously published high-resolution multi-parameter 7T structural MRI data [1].

Supplementary material 1) A Jupyter Notebook containing all the Python (V3.6) code used to pre-process the DWI data [12,13]. The notebook is also shared on OSF (DOI [10.17605/OSF.IO/ZVXHW](https://doi.org/10.17605/OSF.IO/ZVXHW)).

Supplementary material 2) A Microsoft Excel file containing the MRI exam card parameters. The excel file is also shared on OSF (DOI [10.17605/OSF.IO/ZVXHW](https://doi.org/10.17605/OSF.IO/ZVXHW)).

2. Experimental Design, Materials and Methods

Participants Each healthy participant had previously participated in a structural 7Tesla (T) magnetic resonance imaging (MRI) session as described in [1] and were recruited via newsletters and social media of the Dutch Parkinson Foundation, as well as via the University of Amsterdam. The larger data-collection effort entailed two 7T MRI sessions and a third 3T MRI session. All participants were contacted by phone to assess their suitability to participate in the study. Initial inclusion criteria for the first 7T MRI scan were age 18–80 years and self-reported health at the time of inclusion. Exclusion criteria were the absence of a signed informed consent, as well as any factors that could potentially interfere with MRI. This included MRI incompatibility (e.g., pacemakers), pregnancy, and self-reported claustrophobia. All exclusion criteria were verified again before the 3T MRI session commenced. The interval between the first 7T structural MRI session and the 3T DWI MRI session was on average 2.35 years (std. 0.23; the minimum and maximum interval was resp. 1.66 and 3.15 years). The age group membership as reported

in Table 1 is based on the age at diffusion-weighted data acquisition and could therefore differ from the age group in the initial 7 Tesla structural data release. Each participant received a monetary compensation of 20 euros. Of the initial 54 participants there were five participants for whom the data was not fully exported, or the exported data was corrupted. These five participants were excluded from any further data processing.

Data acquisition summary The data were acquired using a Philips 3T Ingenia CX scanner with a dStream 32 channel receiver head coil at the Spinoza Center for Neuroimaging located in Amsterdam, The Netherlands (<https://www.spinozacentre.nl>). The scanner has a maximum gradient strength of 40mT/m and a maximum gradient slew rate of 200 mT/m/ms. The diffusion weighted images were acquired with a multislice spin echo (MS-SE), single-shot sequence (100 transverse slices with an isotropic voxel resolution of 1.28mm, field of view (FOV) = 205 × 205, slice gap = 0mm, TR = 8100ms, TE = 78ms, SENSE factor (AP) = 2). To suppress the fat signal two REST saturation slabs were planned at the anterior and posterior side of the brain. Diffusion weighting was isotropically distributed along 48, 56, or 64 directions with a corresponding b-value of 700 s/mm², 1000 s/mm² and 1600 s/mm². Due to memory limitations the 64-direction scan was split into two 32 direction scans (resp. TA b700= 13:48min, b1000 = 17:19min, b1600 first half = 9:44 min, b1600 second half = 9:44 min). Each diffusion weighted image included several volumes with no diffusion weighting (b₀; b value = 0 s/mm²). The b700 scan started and ended with a b₀ volume, the b1000 scan started with a single b₀ volume and ended with five b₀ volumes, the first half of the b1600 scan started and ended with a single b₀, whereas the second half of the b1600 scan started with a single and ended with two b₀ volumes. In total twelve b₀ volumes were acquired within the diffusion weighted sequences. Finally, eight b₀ volumes were acquired with an inverted fat shift direction to ensure that *topup* could be used (100 transverse slices with an isotropic voxel resolution of 1.28mm, field of view (FOV) = 205 × 205, slice gap = 0mm, TR = 8100ms, TE = 78ms, SENSE factor (AP) = 2, TA single b₀ volume = 00:49 min). Note that the exact exam card and corresponding MRI parameters are presented in Supplementary file 2 ('MRI examcard parameters.xlsx').

Data pre-processing Of the 49 participants, the DWI data were saved using a DICOM format for three participants and PAR/REC format for 46 participants. Depending on the format, the data was exported to the NIfTI format using *dcm2niix* (V1.0.20201216) or *parrec2nii* (V3.2.1) [2,3] and converted to the MRtrix3 .mif format [4]. The DWI and b₀ files used for the *topup* were concatenated into separate .mif files for ease of processing. No intensity normalization was done prior to concatenation. All data were subsequently denoised using a principle component analysis (PCA) based function *dwidenoise* as implemented in MRtrix3 (V3.0.2) [4,5,14]. This function denoises the DWI data using the prior knowledge that the eigen spectrum of random covariance matrices can be described by a Marchenko-Pastur (MP) distribution. A MP distribution is fit to the spectrum of patch-wise signal matrices and used as an estimator of the amount of noise. This noise estimation is then used as an optimal cut-off for the PCA denoising. The next step was to remove the Gibbs ringing artefacts by using the *mrdegibbs* function [4,6]. Gibbs-ringing can be seen in MRI images as spurious oscillations around sharp tissue boundaries and is a result of the truncation of k-space sampling. Depending on the location of this sharp edge relative to the sampling grid this results in the attenuation of the Gibbs ringing artifact. The used method tries to estimate the subvoxel-shift in pixels necessary to minimize this distance and re-interpolates the image accordingly. The next step was to correct for susceptibility-induced off-resonance field distortions using the different phase encoding blips of the b₀ images in *topup*. The *topup* output was used to inform the eddy current correction using *eddyOpenMP* as implemented in FSL (V5.0.11) [7–9,15]. Finally, we applied a N4 bias correction as implemented in *dwibiascorrect* [4,10] and a brain mask was estimated using *dwi2mask* [11]. The bias field is the result of the inhomogeneity of the magnetic field during acquisition and has a negative effect on any intensity-based segmentation. All DWI volumes were finally exported back to NIfTI format using *mrconvert* with the option *export_grad_fsl* to export the bvals and bvects files in a FSL compatible format. All facial features were removed from the resulting NIfTI file using the brain mask in combination with *fslmaths*. The processing pipeline is visualized in Fig. 1. The final DWI NIfTI image contains 180 volumes, of which twelve are the b₀ (posterior fat shift direction)

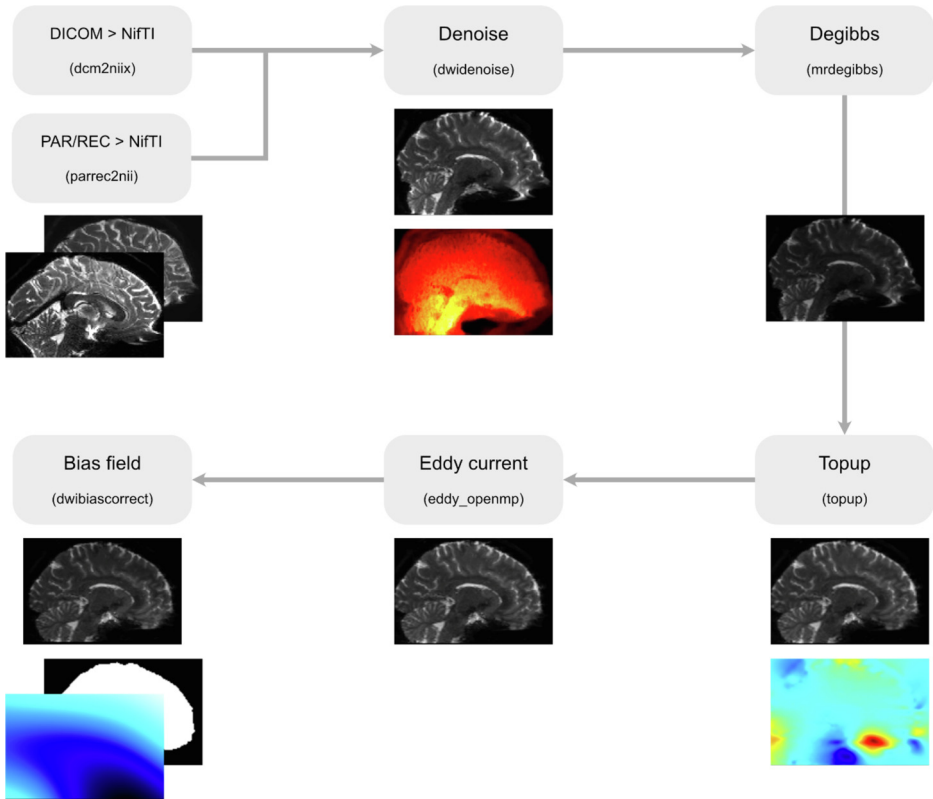


Fig. 1. DWI pre-processing steps. The DWI scans were either saved as DICOM or PAR/REC format. Depending on the format, the data was exported to the NIFTI format using either `dcm2nii` or `parrec2nii` [2,3] and converted to the MRtrix3 `.mif` format [4]. All data were then denoised using `dwidenoise` [5]. A corresponding noise map is shown in red. The next step was to remove the Gibbs ringing artefacts by using the `mrdegibbs` function [6]. Using the different phase encoding blips of the `b0` images, `topup` was applied and used to inform the eddy current correction as implemented in FSL [7–9]. A custom `b02b0.cnf` parameter script was used during the `topup` processing step in which the warp resolution was increased, and the amount of smoothing was reduced. This custom script is generated as part of the processing code shared in supplementary material 1 (‘A high-resolution multi-shell 3T diffusion magnetic resonance imaging dataset as part of the Amsterdam Ultra-high field adult lifespan database (AHEAD)_notebook.ipynb’, cell 6). The estimated susceptibility-induced off-resonance field distortions are shown in jet colors. Finally, we applied a N4 bias correction as implemented in `dwibiascorrect` [10] and a brain mask was estimated using `dwi2mask` [11]. All DWI volumes were masked using the resulting brain mask to remove any facial features of the participant. The resulting bias field is given in blue, and the resulting binary brain mask is given in white. In between parentheses are the exact functions used to process the data.

volumes. The remaining volumes are part of the 48, 56 and 64 directional volumes. All code to process the data is provided in a Jupyter notebook [12] as part of the Supplementary material 1. [Figure 2](#)

The 3T MRI data can be combined with the previously published 7T structural MRI data [1]. Note that for two participants the 7T structural MRI data of the first session were deemed unusable and were not part of the initial 7T MRI data release. For those participants the structural scans of the second 7T session will be made available in a future data release.

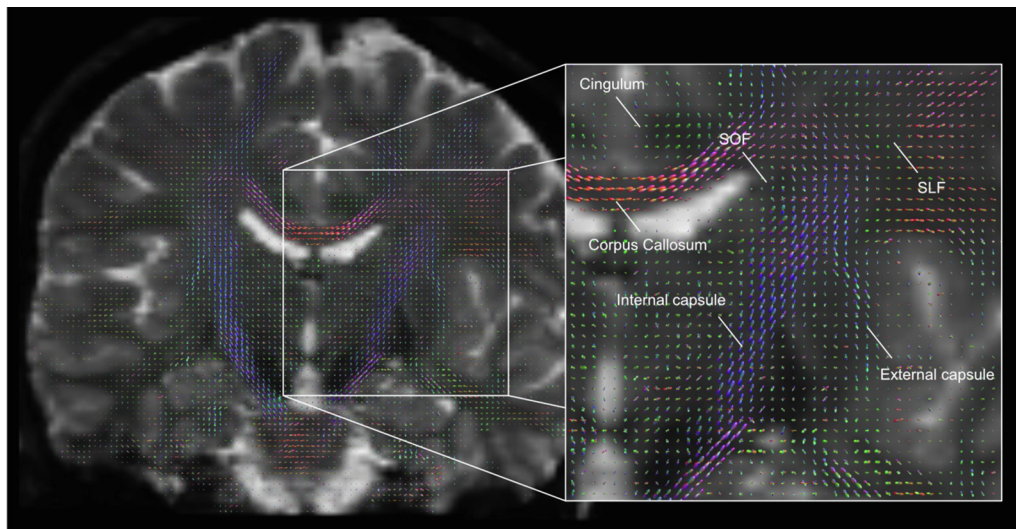


Fig. 2. Visualization of data quality. To visualize the quality of the diffusion data, the freely available pre-processed dataset of a single participant was further analysed with MRtrix3.0. Here, the Fibre Orientation Density (FOD) image of a single coronal slice is shown. The zoomed inset of the basal ganglia illustrates the anatomical specificity captured in the acquired data. The internal and external capsule are clearly visible as well as several other fibre bundles such as the cingulum, corpus callosum, Superior Occipitofrontal Fasciculus (SOF), and the Superior Longitudinal Fasciculus (SLF). The red hues indicate a main orientation along the left/right axis, the green hues indicate a main orientation along the anterior/posterior axis, and the blue hues indicate a main orientation along the superior/inferior axis.

Ethics Statement

All procedures were in accordance with the Code of Ethics of the World Medical Association and approved by the Institutional Review Board at the University of Amsterdam (ERB number 2016-DP-6897). Informed consent was obtained from participants including permission for the future release of de-identified data. In agreement with the general data protection regulation (GDPR), and associated guidelines implemented at the University of Amsterdam, the Netherlands, all information that could be used to directly identify a participant was removed from the data (e.g., the exact age, facial features, and any personal information in the MRI header information). In line with these guidelines we therefore report age ranges, instead of the age of the individual participants. The participant IDs were further pseudorandomized in a similar manner as the AHEAD 7T structural MRI scans. This was done as an additional safety measure to ensure that there is no direct correspondence between the IDs stored locally on the university servers and the IDs shared on figshare. Note that due to GDPR regulations the subject IDs on figshare will differ between releases. The initial 7T AHEAD data release therefore has a different subject ID mapping than the current release. The release version is captured in the subject ID where the first integer indicates the release (0: initial 7T AHEAD data release; 1: current data release including the 3T DWI).

CRedit Author Statement

Max C. Keuken: Software, Formal analysis, Data Curation, Writing – Original Draft, Visualization **Luka C. Liebrand:** Methodology, Investigation, Writing – Review & Editing **Pierre-Louis Bazin:** Conceptualization, Software, Writing – Review & Editing **Anneke Alkemade:** Conceptualization, Supervision, Project administration, Writing – Review & Editing, Funding acquisition **Nikita van Berendonk:** Investigation, Data Curation, Writing – Review & Editing **Josephine M. Groot:** Investigation, Data Curation, Writing – Review & Editing **Scott J.S. Isherwood:** Validation, Writing – Review & Editing **Sarah Kemp:** Validation, Writing – Review & Editing **Nicky Lute:** Investigation, Data Curation, Writing – Review & Editing **Martijn J. Mulder:** Conceptualization, Supervision, Project administration, Writing – Review & Editing, Funding acquisition **Anne C. Trutti:** Validation, Writing – Review & Editing **Matthan W.A. Caan:** Methodology, Investigation, Writing – Review & Editing **Birte U. Forstmann:** Conceptualization, Resources, Supervision, Project administration, Writing – Review & Editing, Funding acquisition.

Declaration of Competing Interest

Of the authors, M.W.A. Caan is shareholder of Nico.lab International Ltd. The other authors declare that they have no known competing financial interests or personal relationships which have or could be perceived to have influenced the work reported in this article. The data described here was acquired with financial support from STW/NWO (#14017, BUF, MJM and AA), Health~Holland TKI-PPP (LL, MWAC), ERC Consolidator (BUF), ERC PoC (BUF), and the NWO Vici (BUF).

Data Availability

[A high-resolution multi-shell 3T diffusion magnetic resonance imaging dataset as part of the Amsterdam Ultra-high field adult lifespan database \(AHEAD\) \(Original data\) \(uvaauas.figshare.com\).](#)

Acknowledgments

The authors thank all individuals that agreed to participate in this study.

Supplementary Materials

Supplementary material associated with this article can be found in the online version at doi:[10.1016/j.dib.2022.108086](https://doi.org/10.1016/j.dib.2022.108086).

References

- [1] A. Alkemade, M.J. Mulder, J.M. Groot, B.R. Isaacs, N. van Berendonk, N. Lute, S.J. Isherwood, P.-L. Bazin, B.U. Forstmann, The Amsterdam Ultra-high field adult lifespan database (AHEAD): A freely available multi-modal 7 Tesla submillimeter magnetic resonance imaging database, *Neuroimage* 221 (2020) 117200, doi:[10.1016/j.neuroimage.2020.117200](https://doi.org/10.1016/j.neuroimage.2020.117200).
- [2] X. Li, P.S. Morgan, J. Ashburner, J. Smith, C. Rorden, The first step for neuroimaging data analysis: DICOM to NIFTI conversion, *J. Neurosci. Methods* 264 (2016) 47–56, doi:[10.1016/j.jneumeth.2016.03.001](https://doi.org/10.1016/j.jneumeth.2016.03.001).
- [3] Brett, Matthew, Markiewicz, Christopher J., Hanke, Michael, Côté, Marc-Alexandre, Cipollini, Ben, McCarthy, Paul, Jarecka, Dorota, Cheng, Christopher P., Halchenko, Yaroslav O., Cottaar, Michiel, Larson, Eric, Ghosh, Satrajit, Wassermann, Demian, Gerhard, Stephan, Lee, Gregory R., Wang, Hao-Ting, Kastman, Erik, Kaczmarczyk, Jakub, Guidotti, Roberto, Duek, Or, Daniel, Jonathan, Rokem, Ariel, Madison, Cindee, Moloney, Brendan, Morency, Félix C., Goncalves, Mathias, Markello, Ross, Riddell, Cameron, Burns, Christopher, Millman, Jarrod, Gramfort, Alexandre, Leppäkangas, Jaakko, Sólón, Anibal, van den Bosch, Jasper J.F., Vincent, Robert D., Braun, Henry, Subramaniam, Krish, Gorgolewski, Krzysztof J., Raamana, Pradeep Reddy, Klug, Julian, Nichols, B. Nolan, Baker, Eric M., Hayashi, Soichi, Pinsard, Basile, Haselgrove, Christian, Hymers, Mark, Esteban, Oscar, Koudoro, Serge, Pérez-García, Fernando, Oosterhof, Nikolaas N., Amirbekian, Bago, Nimmo-Smith, Ian, Nguyen, Ly, Reddigari, Samir, St-Jean, Samuel, Panfilov, Egor, Garyfallidis, Eleftherios, Varoquaux, Gael, Legarreta, Jon Haitz, Hahn, Kevin S., Hinds, Oliver P., Fauber, Bennet, Poline, Jean-Baptiste, Stutters, Jon, Jordan, Kesshi, Cieslak, Matthew, Moreno, Miguel Estevan, Haenel, Valentin, Schwartz, Yannick, Baratz, Zvi, Darwin, Benjamin C., Thirion, Bertrand, Gauthier, Carl, Papadopoulos Orfanos, Dimitri, Solovey, Igor, Gonzalez, Ivan, Palasubramaniam, Jath, Lecher, Justin, Leinweber, Katrin, Raktivan, Konstantinos, Calábková, Markéta, Fischer, Peter, Gervais, Philippe, Gadde, Syam, Ballinger, Thomas, Roos, Thomas, Reddam, Venkateswara Reddy, Freec84, nipy/nibabel: 3.2.1, Zenodo, 2020. <https://doi.org/10.5281/ZENODO.4295521>.
- [4] J.-D. Tourmier, R. Smith, D. Raffelt, R. Tabbara, T. Dhollander, M. Pietsch, D. Christiaens, B. Jeurissen, C.-H. Yeh, A. Connelly, MRtrix3: A fast, flexible and open software framework for medical image processing and visualisation, *Neuroimage* 202 (2019) 116137, doi:[10.1016/j.neuroimage.2019.116137](https://doi.org/10.1016/j.neuroimage.2019.116137).
- [5] J. Veraart, D.S. Novikov, D. Christiaens, B. Ades-aron, J. Sijbers, E. Fieremans, Denoising of diffusion MRI using random matrix theory, *Neuroimage* 142 (2016) 394–406, doi:[10.1016/j.neuroimage.2016.08.016](https://doi.org/10.1016/j.neuroimage.2016.08.016).
- [6] E. Kellner, B. Dhital, V.G. Kiselev, M. Reisert, Gibbs-ringing artifact removal based on local subvoxel-shifts: Gibbs-Ringing Artifact Removal, *Magn. Reson. Med.* 76 (2016) 1574–1581, doi:[10.1002/mrm.26054](https://doi.org/10.1002/mrm.26054).
- [7] J.L.R. Andersson, S.N. Sotiropoulos, An integrated approach to correction for off-resonance effects and subject movement in diffusion MR imaging, *Neuroimage* 125 (2016) 1063–1078, doi:[10.1016/j.neuroimage.2015.10.019](https://doi.org/10.1016/j.neuroimage.2015.10.019).
- [8] S.M. Smith, M. Jenkinson, M.W. Woolrich, C.F. Beckmann, T.E.J. Behrens, H. Johansen-Berg, P.R. Bannister, M. De Luca, I. Drobnjak, D.E. Flitney, R.K. Niazy, J. Saunders, J. Vickers, Y. Zhang, N. De Stefano, J.M. Brady, P.M. Matthews, Advances in functional and structural MR image analysis and implementation as FSL, *Neuroimage* 23 (2004) S208–S219, doi:[10.1016/j.neuroimage.2004.07.051](https://doi.org/10.1016/j.neuroimage.2004.07.051).
- [9] J.L.R. Andersson, S. Skare, J. Ashburner, How to correct susceptibility distortions in spin-echo echo-planar images: application to diffusion tensor imaging, *Neuroimage* 20 (2003) 870–888, doi:[10.1016/S1053-8119\(03\)00336-7](https://doi.org/10.1016/S1053-8119(03)00336-7).
- [10] N.J. Tustison, B.B. Avants, P.A. Cook, Yuanjie Zheng, A. Egan, P.A. Yushkevich, J.C. Gee, N4ITK: Improved N3 Bias Correction, *IEEE Trans. Med. Imaging* 29 (2010) 1310–1320, doi:[10.1109/TMI.2010.2046908](https://doi.org/10.1109/TMI.2010.2046908).
- [11] T. Dhollander, D. Raffelt, A. Connelly, in: *Unsupervised 3-tissue response function estimation from single-shell or multi-shell diffusion MR data without a co-registered T1 image*, ISMRM Workshop on Breaking the Barriers of Diffusion MRI, Lisbon, Portugal, 2016, p. 5.
- [12] T. Kluyver, B. Ragan-Kelley, F. Pérez, M. Bussonnier, J. Frederic, J. Hamrick, J. Grout, S. Corlay, P. Ivanov, S. Abdalla, C. Willing, in: *Jupyter Notebooks—a publishing format for reproducible computational workflows*, Positioning and Power in Academic Publishing: Players, Agents and Agendas, Göttingen, Germany, 2016, p. 4.
- [13] G. van Rossum, J. de Boer, Interactively testing remote servers using the Python programming language, *CWI Quarterly* 4 (1991) 283–304.
- [14] L. Cordero-Grande, D. Christiaens, J. Hutter, A.N. Price, J.V. Hajnal, Complex diffusion-weighted image estimation via matrix recovery under general noise models, *Neuroimage* 200 (2019) 391–404, doi:[10.1016/j.neuroimage.2019.06.039](https://doi.org/10.1016/j.neuroimage.2019.06.039).
- [15] M.S. Graham, I. Drobnjak, M. Jenkinson, H. Zhang, Quantitative assessment of the susceptibility artefact and its interaction with motion in diffusion MRI, *PLoS One* 12 (2017) e0185647, doi:[10.1371/journal.pone.0185647](https://doi.org/10.1371/journal.pone.0185647).